Biomedicine & Pharmacotherapy 191 (2025) 118463

Contents lists available at ScienceDirect

Biomedicine & Pharmacotherapy

journal homepage: www.elsevier.com/locate/biopha

Cannabigerol attenuates liver fibrosis via AMPK activation: Regulation of lipid metabolism, inflammation, and hepatic stellate cell activation

Kyung-Hwa Jeon [a,b,c], Seojeong Kim [a], Seojeong Park [a], Eun Seon Pak [a,b], Soomin Kim [d,e], Hwa Jong Lee [d,e], Tae Hyung Kim [d,e], Jun Jie Piao [d], Dongho Shin [d], Woong Jin Bae [c,d], Sae Woong Kim [c,d,f], Youngjoo Kwon [a,b,*]

[a] College of Pharmacy & Graduate School of Pharmaceutical Sciences, Ewha Womans University, Seoul 03760, Republic of Korea
[b] Graduate Program in Innovative Biomaterials Convergence, Ewha Womans University, Seoul 03760, Republic of Korea
[c] Catholic Integrative Medicine Research Institute, The Catholic University of Korea, Seoul 06591, Republic of Korea
[d] Department of Urology, College of Medicine, The Catholic University of Korea, Seoul 06591, Republic of Korea
[e] Department of Biomedical Sciences, College of Medical Sciences, The Catholic University of Korea, Seoul 06591, Republic of Korea
[f] Green Medicine Co., Ltd, Busan 48307, Republic of Korea

ARTICLE INFO

Keywords:
Phytocannabinoid
Cannabigerol (CBG)
Liver fibrosis
AMP-activated protein kinase (AMPK)

ABSTRACT

Liver fibrosis, driven by lipid dysregulation and chronic inflammation, remains a major global health burden with limited therapeutic options. This study investigates the therapeutic potential of cannabigerol (CBG), a minor non-psychoactive phytocannabinoid, in mitigating hepatic lipid accumulation and inflammation. In hepatocytes exposed to palmitic and oleic acids (PA/OA), CBG significantly reduced lipid accumulation by suppressing lipogenesis and enhancing lipophagy. Mechanistic studies revealed that CBG directly activated AMP-activated protein kinase (AMPK), as confirmed by *in vitro* activity assay and molecular docking study. Additionally, CBG markedly suppressed the expression of pro-inflammatory cytokines (*IL6*, *IL1B*, and *TNFA*) and attenuated the activation of hepatic stellate cells. Importantly, both the lipid-lowering and anti-inflammatory effects of CBG were abolished by co-treatment with the AMPK inhibitor compound C, confirming AMPK as a central mediator of actions of CBG. These findings highlight CBG as a promising therapeutic candidate for liver fibrosis, offering dual modulation of lipid metabolism and inflammatory signaling via AMPK activation.

1. Introduction

Liver fibrosis, a pathological response to chronic liver injury, is frequently driven by excessive lipid accumulation resulting from dysregulated lipid metabolism [1]. This aberrant lipid accumulation triggers inflammatory responses and tissue remodeling, collectively exacerbating disease progression [2,3]. Unlike simple steatosis, liver inflammation plays a pivotal role in the development of fibrosis, underscoring the complex interplay between metabolic dysfunction and inflammatory signaling. Accordingly, targeting dysregulated fatty acid metabolism to prevent lipid accumulation and disrupt the pro-inflammatory microenvironment has emerged as a promising therapeutic strategy [1,4]. Despite ongoing efforts, there remains a significant therapeutic unmet need in the treatment of liver fibrosis, as no approved pharmacological therapies currently exist to reverse or halt disease progression in clinical settings. In response, various therapeutic approaches are being actively explored, including the identification of therapeutic targets [5–7], discovery of targeted delivery approaches [8], and the development of novel therapeutic compounds [9,10]. These efforts reflect the multifactorial nature of liver fibrosis and the need for comprehensive therapeutic interventions.

Cannabinoids derived from *Cannabis sativa* have gained increasing attention due to their diverse pharmacological properties and therapeutic potential for various diseases [11]. Among them, cannabigerol (CBG, Fig. 1A), a non-psychoactive minor phytocannabinoid, has shown distinct biological activities, including antibacterial, antifungal, and anti-inflammatory effects [11]. As a biosynthetic precursor of other cannabinoids, CBG shares structural similarities with other cannabinoid compounds, but possesses unique pharmacological properties that remain largely underexplored [12]. Recent studies have reported that CBG can alleviate liver fibrosis in experimental models, suggesting its potential as a novel [13]. However, the underlying mechanisms by

* Corresponding author at: College of Pharmacy & Graduate School of Pharmaceutical Sciences, Ewha Womans University, Seoul 03760, Republic of Korea.
E-mail address: ykwon@ewha.ac.kr (Y. Kwon).

https://doi.org/10.1016/j.biopha.2025.118463
Received 19 May 2025; Received in revised form 29 July 2025; Accepted 6 August 2025
Available online 15 August 2025
0753-3322/© 2025 The Authors. Published by Elsevier Masson SAS. This is an open access article under the CC BY license (http://creativecommons.org/licenses/by/4.0/).

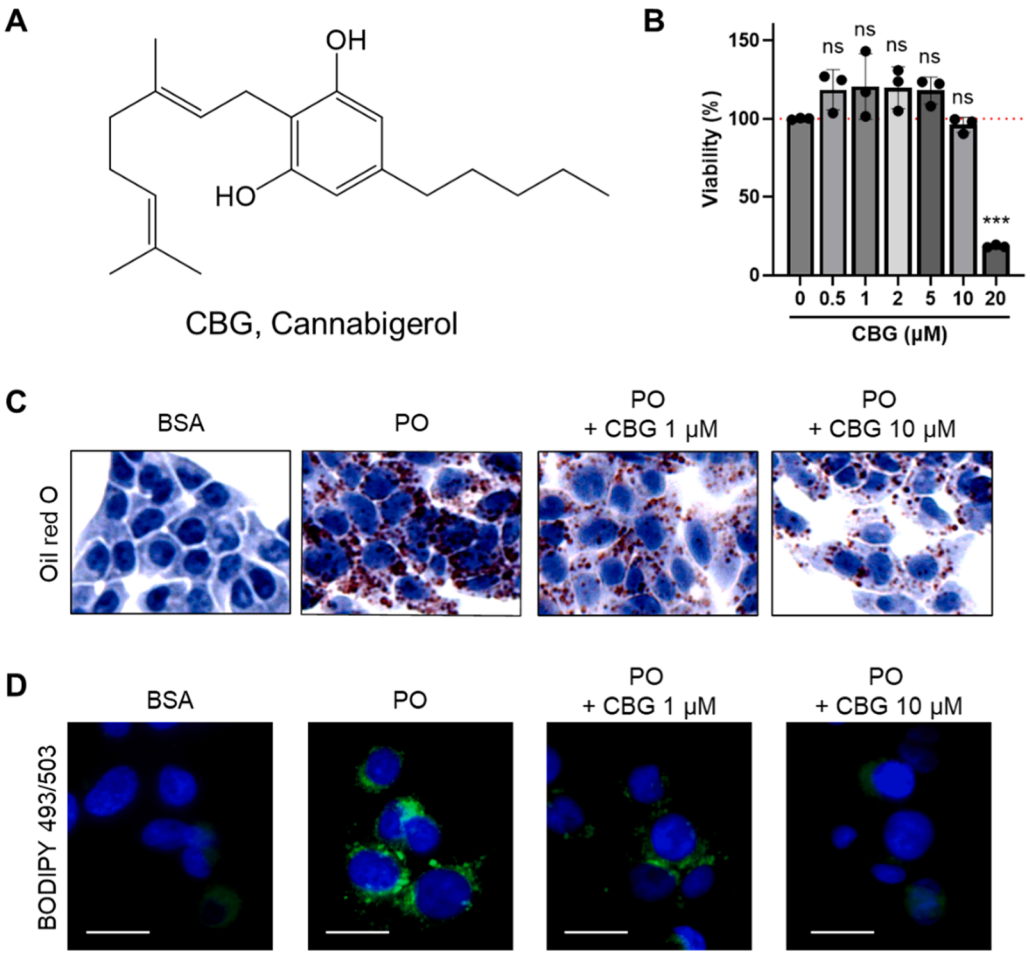


Fig. 1. CBG ameliorated lipid accumulation in hepatocytes. (A) Chemical structure of CBG. (B) WST assay results showing cell viability of HepG2 cells treated with CBG at the indicated concentrations for 24 h. Data are presented as mean ± SD from three independent experiments (n = 3 biological replicates). *p*-Values were determined by one-way ANOVA, followed by Dunnett's multiple comparison test. ***$p < 0.001$; ns., not significant. (C) Oil Red O staining of HepG2 cells exposed to PA/OA with or without CBG (1 or 10 μM) for 4 h. Lipid droplet accumulation was quantified based on Oil Red O staining intensity. (D) Representative images of lipid droplets stained with BODIPY493/503 in HepG2 cells treated with PA/OA alone or in combination with CBG (0, 1, or 10 μM). Scale bar = 20 μm.

which CBG exerts these effects are not fully understood, necessitating further research to elucidate its mode of action and therapeutic pathways.

AMP-activated protein kinase (AMPK), a key regulator of cellular energy homeostasis, plays a central role in lipid metabolism and modulates pathways involved in fibrosis and inflammation [14–16]. These multifaceted roles make AMPK an attractive target for the treatment of liver diseases. However, current pharmacological strategies, such as the use of metformin, an indirect AMPK activator, are limited by suboptimal efficacy and translational applicability [17,18]. Therefore, there is an urgent need to identify novel compounds capable of directly activating AMPK with therapeutic efficacy in relevant models of liver disease.

In this study, we investigated the potential of CBG to attenuate hepatic lipid accumulation by regulating lipogenesis and promoting lipophagy in hepatocytes. CBG was found to suppress inflammatory signaling and inhibit HSC activation. Mechanistically, the lipid-lowering and anti-inflammatory effects of CBG were mediated by AMPK activation, as demonstrated by *in vitro* assays, *in silico* docking analysis, and reversal of these effects by compound C, an AMPK inhibitor. These findings highlight CBG as a novel therapeutic candidate for metabolic-associated steatohepatitis (MASH) and related liver diseases, and also provide valuable insights for cannabinoid-based therapeutic strategies.

2. Materials and methods

2.1. Cell culture drug treatment

The human hepatocyte cell line HepG2 was obtained from ATCC and cultured in Minimum Essential Medium (MEM, Welgene, Korea) supplemented with 10 % fetal bovine serum (FBS, Hyclone, USA). Cells were maintained at 37°C in a humidified atmosphere with 5 % CO_2.

To assess lipid accumulation in hepatocyte, HepG2 cells were treated with a mixture of palmitic acid and oleic acid (PA/OA, 0.5/1 mM) in complete medium for 4 h. Control cells received bovine serum albumin (BSA) instead of PA/OA. CBG (1 or 10 μM) was co-treated with PA/OA to evaluate its effects on lipid metabolism. To determine the involvement of AMPK, cells were co-treated with compound C (10 μM), an AMPK inhibitor.

2.2. WST assay

Cell viability was assessed using the WST assay. HepG2 cells (1×10^4 cells/well) were seeded in a 96-well cell culture plate and treated with various concentrations of CBG in a total volume of 100 μL per well for 24 h. The control group received MEM containing an equivalent volume of DMSO. All treatments were performed in triplicate. After incubation, WST solution (Quanti-Max™, Biomax, Korea) was added to each well and incubated according to the manufacturer's protocol, and

Table 1
Primer sequences used in this study.

Gene		Sequence
PPARG	Forward	5'-TACTGTCGGTTTCAGAAATGCC−3'
	Reverse	5'-GTCAGCGGACTCTGGATTCAG−3'
FASN	Forward	5'-ACAGCGGGGAATGGGTACT−3'
	Reverse	5'-GACTGGTACAACGAGCGGAT−3'
SCD1	Forward	5'-TCATAATTCCCGACGTGGCT−3'
	Reverse	5'-CCCAGAAATACCAGGGCACA−3'
PPARA	Forward	5'-GTCATCACGGACACGCTTTCA−3'
	Reverse	5'-CGGTCGCACTTGTCATACAC−3'
PPARGC1A	Forward	5'-GTA AATCTGCGGGATGATGG−3'
	Reverse	5'-ATTGCTTCCGTCCACAAA A−3'
IL6	Forward	5'-GAGTAGTGAGGA ACA AGCCAG A−3'
	Reverse	5'-AAGCTGCGCAGAATGAGATGA−3'
IL1B	Forward	5'-ACAGATGAAGTGCTCCTTCCA−3'
	Reverse	5'-GTCGGAGATTCGTAGCTGGAT−3'
TNFA	Forward	5'-TGGCGTGGAGCTGAGAGATA−3'
	Reverse	5'-TGATGGCAGAGAGGAGGTTG−3'
GAPDH	Forward	5'-CTTTGTCAAGCTCATTTCCTGG−3'
	Reverse	5'-TCTTCCTCTTGTGCTCTTGC−3'
COL1A1	Forward	5'-GGACACAGAGGTTTCAGTGG−3'
	Reverse	5'-CCAGTAGCACCATCATTTCC−3'
FN1	Forward	5'-GTGTTGGGAATGGTCGTGGGGAATG−3'
	Reverse	5'-CCAATGCCACGGCCATAGCAGTAGC−3'
ACTA2	Forward	5'-AGTTACGAGTTGCCTGATGG−3'
	Reverse	5'-GAGGTCCTTCCTGATGTCAA−3'

Table 2
Antibody information used in this study.

Antibody	Vendor	Catalogue number	Application
SREBP−1	Santa-cruz	sc−365513	WB
ATG12	Cell Signaling	4180 T	WB
SQSTM1/p62	Cell Signaling	5114	WB
pAMPK	Cell Signaling	2535 s	WB
AMPK	Thermo Fisher	AHO1332	WB
pACC	Cell Signaling	11818 s	WB
ACC	Cell Signaling	3676 s	WB
GAPDH	MBL	M171–3	WB
NF-κB	Cell Signaling	8242	IF
Alexa Fluor 568 rabbit	Thermo Fisher	A11011	IF
α-SMA	Abcam	Ab5694	IF

absorbance was measured at 450 nm using a Multiskan Microplate Reader (Thermo Fisher Scientific, USA).

2.3. Oil red O staining

After treatment, HepG2 cells were washed with PBS and fixed in 4 % paraformaldehyde for 20 min. Cells were then washed with distilled water, stained with 200 μL 60 % Oil red O solution at room temperature, and subsequently washed again with distilled water. Nuclei were counterstained with hematoxylin. Lipid droplet accumulation was visualized using a microscope (Zeiss, Germany).

2.4. Quantitative real-time polymerase chain reaction (qRT-PCR)

Total RNA was extracted using TRIzol reagent (Invitrogen, USA). Reverse transcription was performed using the PrimeScript™ RT Reagent kit (Takara, Japan). qRT-PCR was performed using the SensiFAST™ SYBR No-ROX kit (Bioline, Korea) on CFX96 RT-PCR detection system (Bio-rad, USA). *GAPDH* was used as an internal control, and relative mRNA expression was calculated using the $2^{-\Delta\Delta CT}$ method. Primer sequences used in this study are listed in Table 1.

2.5. Western blot

Total proteins were extracted using RIPA buffer (Cell Signaling Technology, USA) and quantified using a Pierce™ BCA Protein Assay kit (Thermo Fisher Scientific, USA). Equal amounts of protein were separated by SDS-PAGE (10–15 %) and transferred to PVDF membranes (PALL Corp., USA). Membranes were blocked with 5 % skimmed milk or BSA in TBST for 1 h at room temperature, followed by overnight incubation at 4 °C with primary antibodies (listed in Table 2). After washing with TBST, membranes were incubated with HRP-conjugated secondary antibodies for 1 h at room temperature. Protein bands were visualized using enhanced chemiluminescence reagents (Amersham™ ECL Prime, GE Healthcare, USA) and detected with a ChemiDoc MP imaging system (Bio-RAD, USA).

2.6. Immunofluorescence

To assess autophagic induction, cells were cultured on eight-well chamber slides (SPL, Korea) and transfected with the tandem fluorescent reporter plasmid pcDNA3-GFP-LC3-RFP-LC3ΔG (Addgene, #168997) using jetPRIME transfection reagent (Polyplus, France). After 12 h of transient transfection, cells were treated with PA/OA alone or in combination with CBG for 4 h. Cells were then washed with PBS and fixed with 4 % paraformaldehyde. Slides were mounted using ProLong™ Gold antifade reagent containing DAPI (Invitrogen, USA) and covered with coverslips.

To evaluate NF-κB nuclear localization, cells were seeded on eight-well chamber slides and grown to 80 % confluency. After washing with PBS and fixation with 4 % paraformaldehyde, cells were blocked using a solution containing 5 % blocking one-P (Nacalai Tesque, Japan) and 0.1 % triton-X in PBS. Primary antibodies were applied and incubated overnight at 4℃, followed by incubation with secondary antibodies for 1 h at room temperature. Slides were mounted with ProLong™ Gold antifade reagent containing DAPI (Invitrogen, USA) and covered with coverslips.

For fibrosis assessment in a 3D hepatic spheroid model, cells were seeded in 96-well round-bottom culture plate (SPL, Korea). and cultured for 10 days to allow spheroid formation. The spheroids were then treated with PA/OA and/or CBG for 4 h. After treatment, spheroids were fixed with 4 % paraformaldehyde and permeabilized with 1 % Triton X-100 in PBS. Primary antibodies were incubated overnight at 4℃, followed by incubation with DAPI and fluorescent secondary antibodies overnight at 4 °C. Slides were mounted with Faramount Mounting Medium (DAKO, Japan) and covered with coverslips. Fluorescence images were acquired using an Apotome laser-scanning microscope (Zeiss, Germany) and analyzed with Zen pro software (Zeiss, Germany).

2.7. In vitro AMPK activity assay

AMPK activity was assessed using the AMPK Kinase Assay Kit and the ADP-Glo™ Assay Kit (both from Promega, USA), following the manufacturer's instructions. Briefly, AMPK enzyme, SAMS peptide, and ATP were incubated with or without CBG or A769662 (a known AMPK activator) to initiate the kinase reaction. Subsequently, ADP-Glo™ reagent was added to deplete residual ATP. The kinase detection reagent was then applied to convert ADP into ATP. The newly generated ATP was quantified by measuring luminescence from a luciferase-luciferin reaction. Luminescence was measured using an Infinite M200 PRO Microplate Reader (Tecan Group Ltd., Switzerland).

2.8. Docking study

A molecular docking study was conducted to evaluate the interaction between CBG and AMPK. The three-dimensional structure of AMPK was obtained from the Protein Data Bank (PDB ID: 4CFF) [19]. Protein preparation, small molecule preparation, and docking analysis were performed using the Protein Preparation Wizard, LigPrep, and Glide docking module, respectively, within the Maestro Software (Schrödinger, USA). Docking experiments were conducted by targeting the active site defined by the ligand present in the PDB structures.

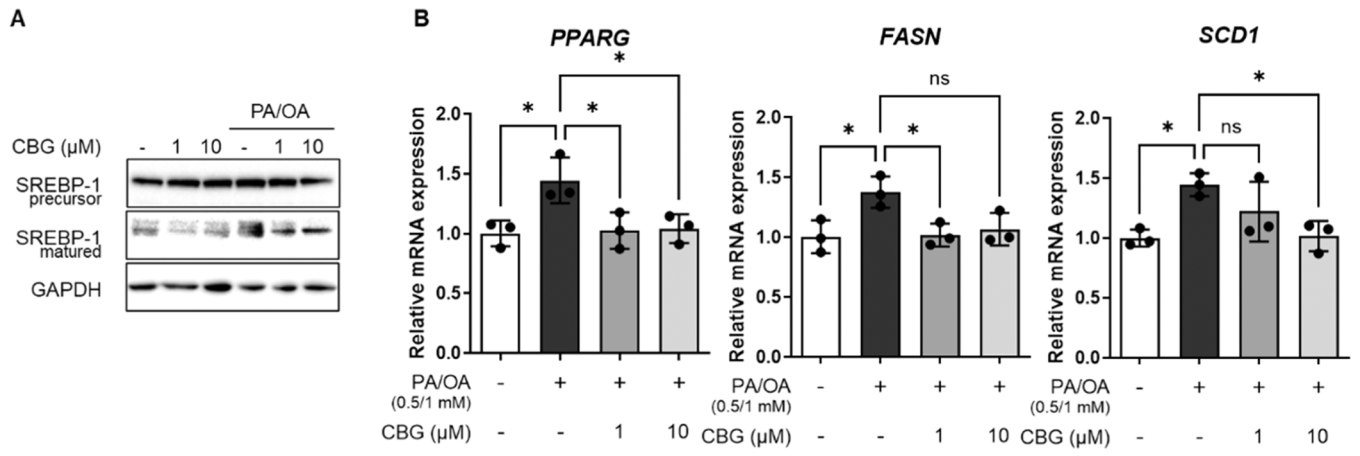


Fig. 2. CBG treatment modulates lipogenesis in PA/OA treated hepatocytes. (A) Representative Western blots of SREBP-1 and GAPDH in HepG2 cells. Three independent experiments were conducted (n = 3 biological replicates), and the corresponding densitometric quantifications are shown below, expressed as relative ratio to the control group (without PA/OA and CBG treatment). (B) Relative mRNA expression levels of lipogenesis-related genes (*PPARG*, *FASN*, and *SCD1*) in HepG2 cells treated with PA/OA in the presence or absence of CBG (1 or 10 μM) for 4 h. *p*-Values were determined by one-way ANOVA, followed by Tukey's multiple comparison test. *$p < 0.05$; ns., not significant. Data are presented as mean ± SD from three independent experiments (n = 3 biological replicates).

2.9. Cytokine array

Cytokine release from hepatocytes was analyzed using the Proteome Profiler Human XL Cytokine Array (R&D Systems, USA). Following treatment with PA/OA alone and in combination with CBG for 4 h, the culture medium was replaced with serum-free medium, and cells were incubated for an additional 12 h. The conditioned medium was collected, centrifugated to remove debris, aliquoted, and stored at −20°C until analysis. The cytokine array was performed using the prepared conditioned medium according to the manufacturer's instructions.

2.10. Statistical analysis

All statistical analyses were conducted using GraphPad Prism 10.0.0 software (GraphPad Software, USA). Data are presented as mean ± standard deviation (SD). Comparisons between two groups were performed using a two-tailed Student's *t*-test, while comparisons involving more than two groups were analyzed using one-way ANOVA, followed by a multiple comparison test. A p-value of less than 0.05 ($p < 0.05$) was considered statistically significant.

3. Results

3.1. CBG treatment ameliorated lipid accumulation in hepatocytes

The cytotoxicity of CBG (Fig. 1A) in HepG2 cells was first assessed to determine a safe working concentration range. Treatment with CBG at concentrations of 0–10 μM for 24 h showed no significant effect on cellular viability (Fig. 1B), but demonstrated a protective effect, as evidenced by reduced levels of cleaved PARP, a marker of apoptosis (Supplementary Figure S1). To investigate the mechanism underlying the previously reported therapeutic effects of CBG in a NAFLD mouse model [13], we evaluated its efficacy in reducing lipid accumulation in the human hepatocyte cell line HepG2, using BODIPY 493/503 and Oil Red O staining. CBG treatment significantly reduced lipid accumulation compared to PA/OA-treated cells, as demonstrated by both staining methods (Fig. 1C and D).

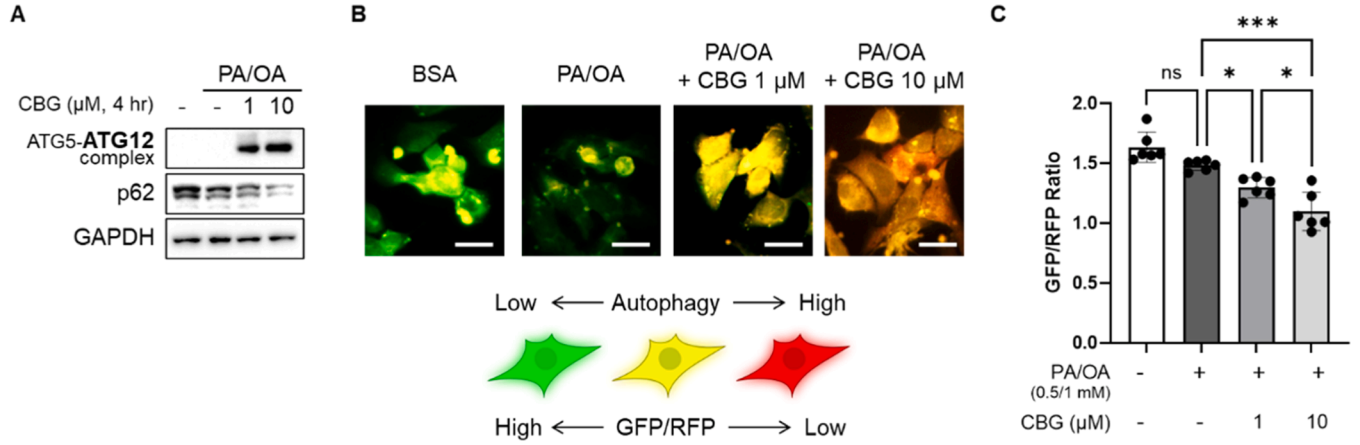


Fig. 3. CBG treatment modulated lipophagy in PA/OA treated hepatocytes. (A) Representative Western blots of ATG5-ATG12 complex, p62, and GAPDH in HepG2 cell lysates. Three independent experiments were conducted (n = 3 biological replicates), and the corresponding densitometric quantifications are shown below, expressed as relative ratio to the control group (without PA/OA and CBG treatment). (B) Representative fluorescence images of GFP-LC3 and RFP-LC3ΔG in transfected HepG2 cells treated with PA/OA in the presence or absence of CBG (1 or 10 μM) for 4 h. Scale bar = 20 μm. (C) Quantification of autophagic flux based on the GFP/RFP fluorescence ratio. *p*-Values were calculated using one-way ANOVA, followed by Tukey's multiple comparison test. *$p < 0.05$; ***$p < 0.001$; ns., not significant. Data are presented as mean ± SD from three independent experiments (n = 3 biological replicates).

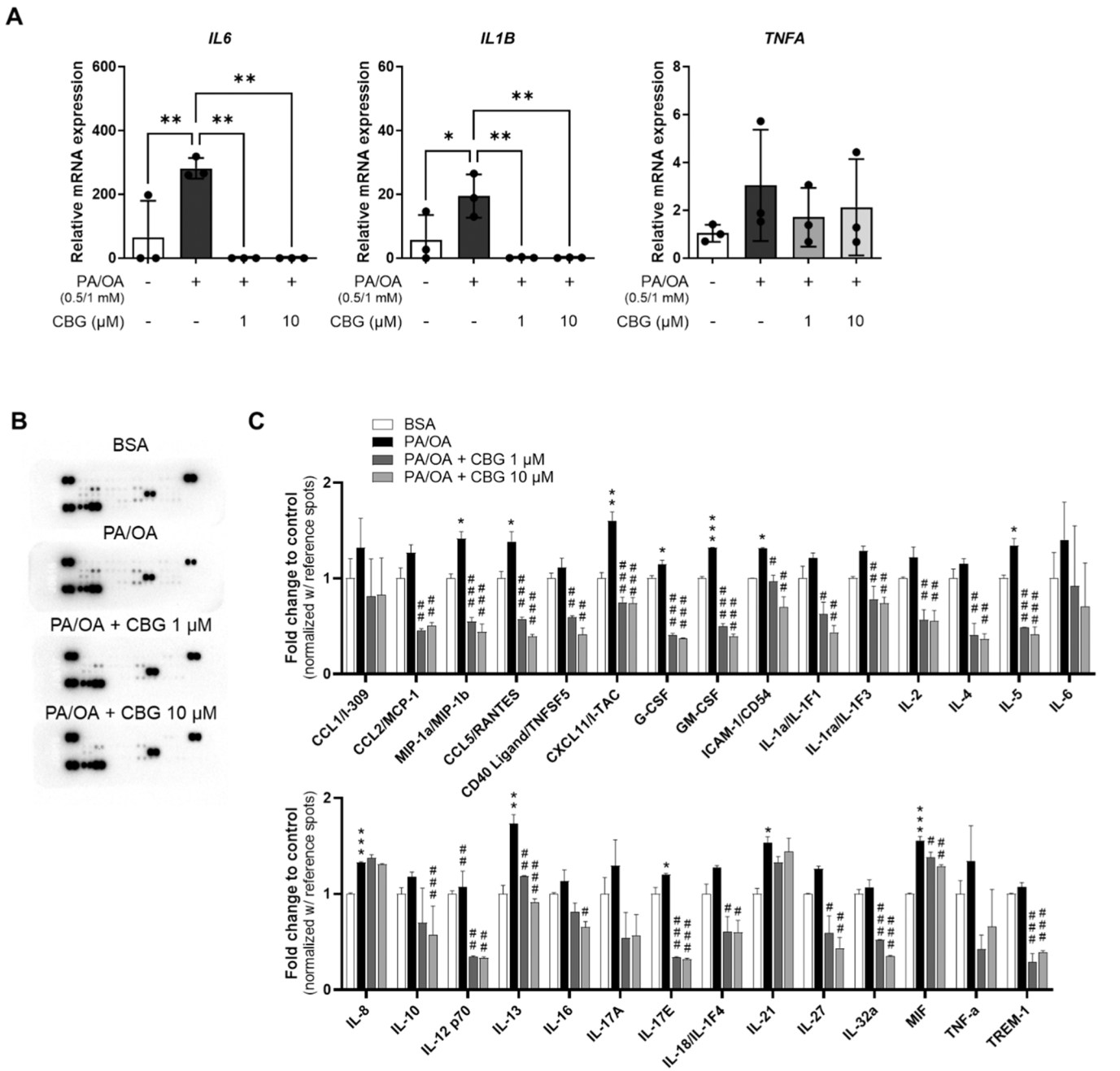


Fig. 4. CBG inhibited inflammatory signaling in PA/OA-treated hepatocytes. (A) Relative mRNA expression levels of inflammation-related genes (*IL6*, *IL1B*, and *TNFA*) in HepG2 cells. *p*-Values were calculated using one-way ANOVA, followed by Tukey's multiple comparison test. $*p < 0.05$; $***p < 0.001$; ns., not significant. Data are presented as mean ± SD from three independent experiments (n = 3 biological replicates). (B) Human cytokine array analysis using conditioned media from HepG2 cells treated with PA/OA and CBG, following a 4-h treatment and subsequent 12-h incubation in serum-free media. (C) Quantitative evaluation of cytokine levels from the array in (B). (A, B) *p*-Values were calculated using one-way ANOVA. $*p < 0.05$; $**p < 0.01$; $***p < 0.001$; ns., not significant (BSA vs. PA/OA); $\#p < 0.05$; $\#\#p < 0.01$; $\#\#\#p < 0.001$; ns., not significant (PA/OA vs. CBG 1 or 10 μM). Data are presented as mean ± SD of two independent densitometric analyses.

3.2. CBG modulated hepatic lipid metabolism by inhibiting lipogenesis and inducing lipophagy

To evaluate whether the effects of CBG on lipid accumulation were mediated through alterations in lipid metabolism, we systematically assessed lipogenesis, lipolysis, and lipophagy in HepG2 cells following CBG treatment. CBG significantly reduced the mature form of SREBP-1, a key regulator of lipid biosynthesis, and downregulated the expression of its downstream effectors, *PPARG*, *FASN*, and *SCD1* (Fig. 2A and B)

To evaluate the influence of CBG on lipolysis, the expression of *PPARA* (encoding PPARα), *PPARGC1A* (encoding PGC1α) and *HSL* (encoding Lipase E) were examined (Supplementary Figure S2 and S3). PA/OA treatment did not significantly suppress *PPARA*, and CBG treatment did not induce notable changes. Although *PPARGC1A* expression showed a slight downward trend with PA/OA and a modest upward trend with low-dose CBG, neither change reached statistical significance.

To assess the role of CBG in promoting lipophagy, a process by which lipid droplets are degraded via autophagy, we analyzed autophagy-related markers. CBG treatment increased ATG5–ATG12 complex

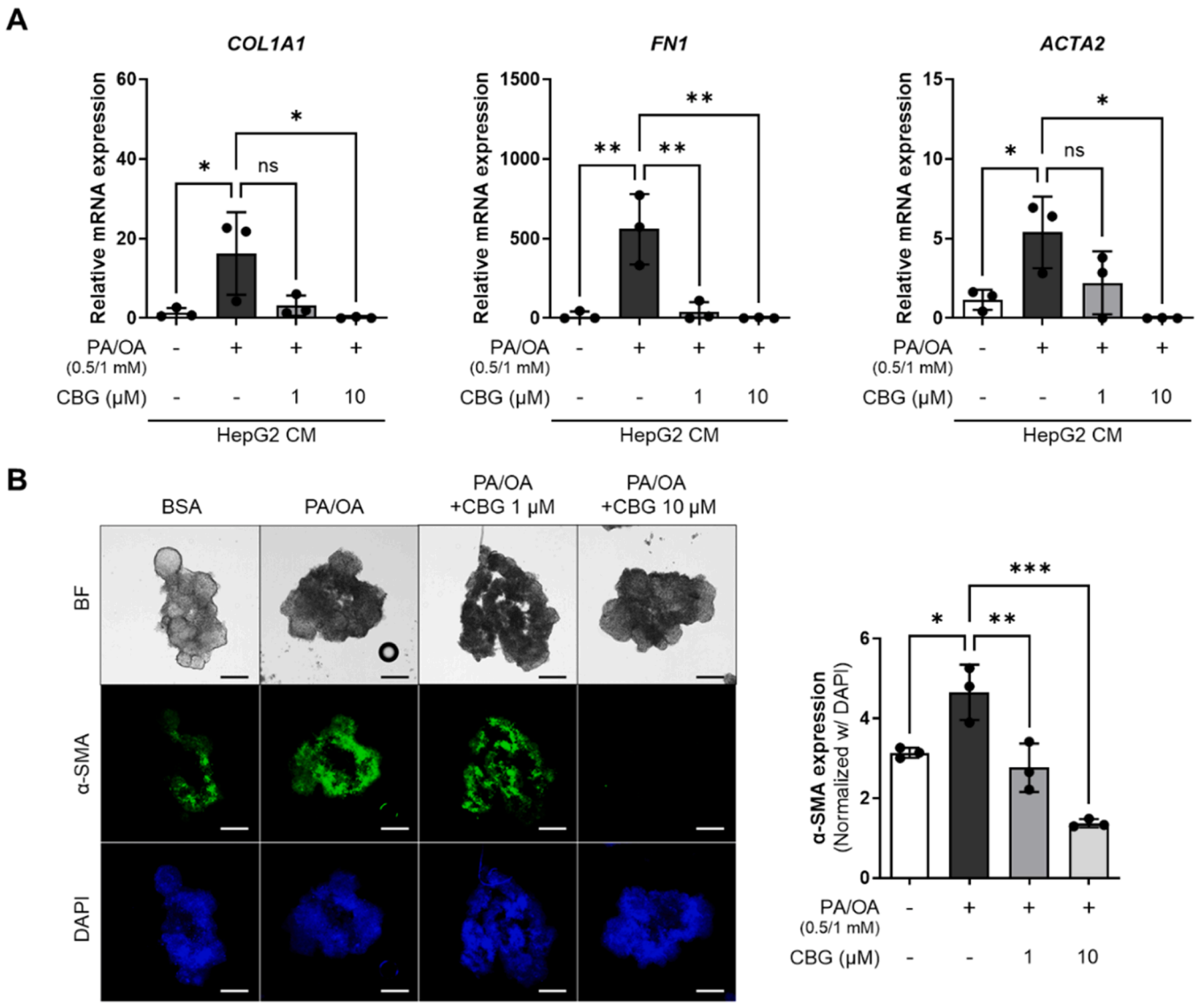


Fig. 5. CBG attenuated fibrogenic response. (A) Relative mRNA expression levels of fibrosis-related genes (*COL1A1*, *FN1*, and *ACTA2*) in LX-2 hepatic stellate cells treated with conditioned media from PA/OA- and CBG-treated HepG2 cells. *p*-Values were calculated using one-way ANOVA, followed by Tukey's multiple comparison test. $*p < 0.05$; $**p < 0.01$; ns., not significant. Data are presented as mean ± SD from three independent experiments (n = 3 biological replicates). (B) Representative fluorescence microscopy images of 3D hepatic spheroids composed of HepG2 and LX-2 cells, stained with anti-α-SMA antibody (1:100). DAPI was used for nucleus counterstaining. Scale bars = 200 μm. (A, B) Data are presented as mean ± SD from a representative experiment of three independent experiments (n = 3 per group). *p*-values were calculated using one-way ANOVA, followed by Tukey's multiple comparison test. $*p < 0.05$; $**p < 0.01$; $***p < 0.001$.

formation and promoted p62 degradation (Fig. 3A). Furthermore, tandem fluorescent LC3 reporter assays showed a decreased GFP/RFP fluorescence ratio, indicative of GFP-LC3 degradation and increased autophagic flux (Fig. 3B and C). These findings suggest that CBG promotes lipid clearance by inhibiting lipogenesis and enhancing lipophagy.

3.3. CBG exerted anti-inflammatory effects by attenuating pro-inflammatory cytokine production and release

As inflammation is a key contributor to liver fibrosis [20], we next assessed the effect of CBG on the link between lipid accumulation and pro-inflammatory cytokine expression in hepatocytes. To determine whether the reduction in lipid accumulation affects cytokine expression, we analyzed the transcript levels of representative pro-inflammatory cytokines, *IL6*, *IL1B* and *TNFA*. PA/OA treatment significantly upregulated the expression of all three cytokines, whereas CBG co-treatment markedly downregulated their mRNA levels (Fig. 4A). To further evaluate cytokine release, a cytokine array analysis was performed using conditioned media collected from HepG2 cells treated with PA/OA and CBG (Fig. 4B, Supplementary Figure S4, and Supplementary Table S1). Densitometric analysis revealed that CBG significantly reduced PA/OA-induced secretion of pro-inflammatory cytokines (Fig. 4C). These data collectively demonstrate that CBG attenuates hepatic inflammation by inhibiting both cytokine production and release.

3.4. CBG attenuated hepatic stellate cell activation and fibrogenesis

To investigate the downstream effects of CBG-mediated anti-inflammatory signaling on fibrogenesis, conditioned media from PA/OA- and CBG-treated HepG2 cells were applied to human hepatic stellate cells (HSCs; LX-2). HSCs play a pivotal role in liver fibrosis, transitioning from a quiescent to an activated state in response to various stimuli, including pro-inflammatory cytokines, thereby promoting extracellular matrix (ECM) deposition and fibrotic progression [4,21]. To examine how the inflammatory signaling changes induced by CBG in hepatocytes

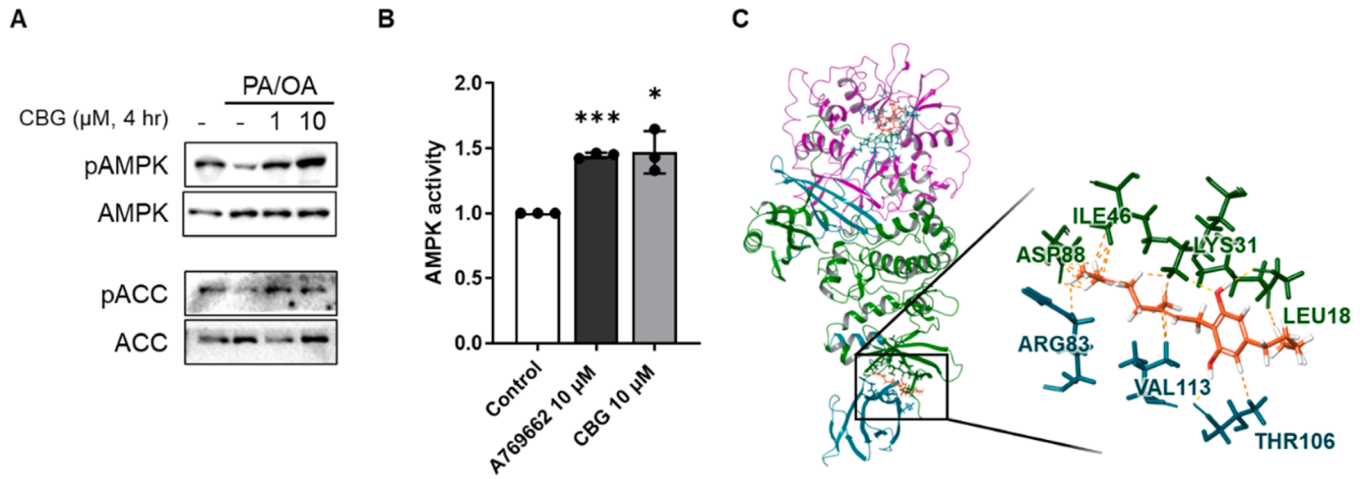


Fig. 6. CBG activated AMPK. (A) Western blot analysis of AMPK signaling pathway proteins in HepG2 cells treated with CBG, showing phosphorylation of AMPK and its downstream target ACC. Three independent experiments were conducted (n = 3 biological replicates), and the corresponding densitometric quantifications are shown below, expressed as relative phosphorylation ratio to the control group (without PA/OA and CBG treatment). (B) *In vitro* AMPK activation by CBG evaluated using an AMPK kinase assay kit, utilizing a SAMS peptide derived from the AMPK substrate and ATP. p-values were calculated using one sample t test: $*p < 0.05$; $***p < 0.001$. Data are presented as mean ± SD from three independent experiments. (C) Docking poses of CBG visualized using Maestro software based on the X-ray crystal structure of AMPK (PDB: 4CFF). The α subunit is shown in green, the β subunit in cyan, and the γ subunit in magenta; CBG is shown in orange. The right panel highlights the interacting residues at the ADaM site.

affect HSC activation, we analyzed the expression of fibrotic markers in LX-2 cells following treatment with conditioned media from PA/OA- and CBG-treated HepG2 cells (Fig. 5A). These results demonstrated that CBG significantly downregulated pro-inflammatory cytokine expression and secretion in PA/OA-treated hepatocytes, which in turn attenuated HSC activation. The expression of α-SMA, a well-established marker of HSC activation [22], was further assessed in a 3D hepatic spheroid model composed of HepG2 and LX-2 cells (24:1 ratio). Consistent with the previous results, CBG treatment significantly reduced α-SMA expression in this model (Fig. 5B), indicating that CBG effectively suppresses HSC activation and ECM accumulation under fibrogenic conditions.

3.5. CBG reduced lipid accumulation via direct AMPK activation

AMPK is a well-known inducer of autophagy [23], and its role in liver fibrosis has been well-documented [9,24]. Previous studies have shown that cannabis extracts containing CBG enhance AMPK phosphorylation in a NAFLD mouse model [25] and that CBG treatment improves liver fibrosis in methionine/choline-deficient diet-induced NASH mice [13].

In our study, AMPK phosphorylation was reduced in PA/OA-treated hepatocytes, but restored by co-treatment with CBG. This CBG-induced AMPK activation was further validated by increased phosphorylation of ACC, a downstream AMPK target (Fig. 6A). *In vitro* AMPK kinase assays confirmed that CBG directly increased AMPK activity to a level comparable to that of A769662, a known direct AMPK activator (Fig. 6B) [26]. To elucidate the mechanism of AMPK activation, we conducted molecular docking analysis using the crystal structure of AMPK (PDB code: 4CFF) and Maestro Software (Schrödinger). The docking results revealed that CBG binds to the ADaM site, a region formed by the catalytic kinase domain of the AMPK α subunit and the regulatory carbohydrate-binding module (CBM) of the AMPK β subunit, in a binding pose similar to that of A769662 [19] (Fig. 6C). CBG interacted with several key residues within these domains: LEU18 (α subunit), LYS31(α subunit), ILE46 (α subunit), ASP88 (α subunit), ARG83 (β subunit), THR106 (β subunit), and VAL113 (β subunit) (Fig. 6C, right panel). These interactions closely resemble the binding profile of known ADaM site-targeting AMPK activators [27]. The docking score for CBG was –4.146, whereas that for the reference AMPK activator A769662 was –6.868. While the docking score of CBG indicates a lower binding affinity that that of A769662, the *in vitro* kinase assay using SAMS peptide revealed that CBG activates AMPK at a comparable level to A769662. Collectively, these findings demonstrated that CBG directly activated AMPK through interaction with the ADaM site, thereby reducing lipid accumulation in hepatocytes.

To verify the AMPK dependency of CBG-induced lipid-lowering effects, we co-treated PA/OA-exposed hepatocytes with CBG and compound C, an AMPK inhibitor. CBG alone significantly reduced lipid droplet accumulation (Fig. 7A), downregulated lipogenic gene expression (Fig. 7B), and enhanced markers of lipophagy (Fig. 7C). These effects were reversed by compound C, confirming that CBG modulates lipid metabolism via its ability to activate AMPK (Fig. 7).

The NF-κB signaling pathway is a highly conserved regulator of inflammatory responses, cell survival, and the progression of hepatocellular injury, liver fibrosis, and hepatocellular carcinoma (HCC) [28]. Importantly, NF-κB activity is mainly regulated by AMPK signaling [29]. Based on this regulatory relationship, we evaluated whether CBG affects NF-κB signaling activation by assessing its nuclear localization in HepG2 cells (Fig. 8). PA/OA treatment induced prominent nuclear translocation of NF-κB, whereas CBG co-treatment effectively suppressed this translocation. Importantly, the inhibitory effect of CBG on NF-κB nuclear localization was reversed by compound C, indicating that anti-inflammatory effects of CBG are mediated via AMPK-dependent inhibition of NF-κB signaling.

4. Discussion

In this study, we systematically evaluated the therapeutic potential of CBG in liver fibrosis, focusing on its effects on lipid metabolism, inflammation, and fibrogenic signaling. Specifically, we demonstrated that CBG effectively regulated lipid metabolism by suppressing lipogenesis and enhancing lipophagy, resulting in reduced lipid accumulation in HepG2 hepatocytes. In addition, CBG exerted potent anti-inflammatory effects by reducing the expression and secretion of pro-inflammatory cytokines, thereby indirectly attenuating HSC activation. Importantly, both the lipid-lowering and anti-inflammatory effects of CBG were mediated through direct activation of AMPK, as evidenced by the reversal of these effects upon co-treatment with compound C, an AMPK inhibitor. Notably, the reduction in cytokine expression was attributed to the AMPK-mediated suppression of NF-κB nuclear translocation, a master regulator of inflammatory signaling.

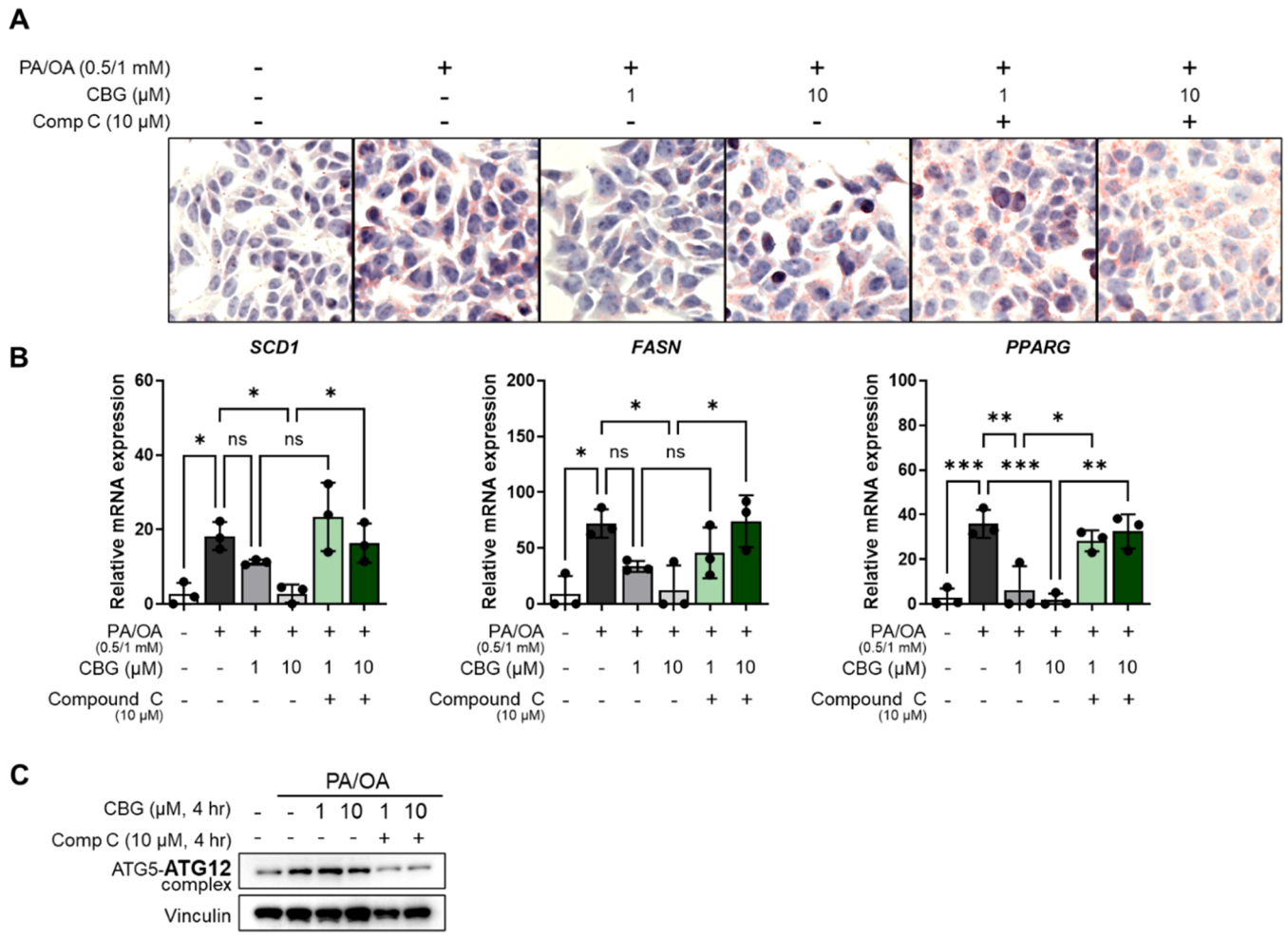


Fig. 7. AMPK inhibition reverses the lipid-lowering effects of CBG. (A) Oil Red O staining of HepG2 hepatocytes exposed to PA/OA in the presence or absence of CBG (1 or 10 μM) and/or compound C for 4 h. Lipid droplet accumulation was quantified based on Oil Red O staining intensity. (B) Relative mRNA expression levels of lipogenesis-related genes (*PPARG*, *FASN*, and *SCD1*) under the same treatment conditions in (A). *p*-values were determined by one-way ANOVA, followed by Tukey's multiple comparison test. $*p < 0.05$; $**p < 0.01$; $***p < 0.001$; ns., not significant. Data are presented as mean ± SD from at least three independent experiments (n = 3 biological replicates). (C) Representative Western blots showing ATG5-ATG12 complex and GAPDH in cellular lysates. Three independent experiments were conducted (n = 3 biological replicates), and the corresponding densitometric quantifications are shown below, expressed as relative ratio to the control group (without PA/OA and CBG treatment).

AMPK plays a critical role in maintaining energy homeostasis and is known to regulate various stages of hepatic fibrosis. It has been reported to attenuate TGF-β signaling and inhibit the expression of profibrotic genes [30,31], as well as to mitigate NF-κB-related inflammatory responses [32,33]. By protecting against inflammatory injury, AMPK activation delays or mitigates the progression of hepatic fibrosis. Previous studies highlighting the role of AMPK in liver fibrosis have demonstrated its involvement not only in hepatocyte lipid metabolism and inflammatory signaling but also in HSC activation. AMPK has been shown to exert potent inhibitory effects on HSC proliferation, migration, and ECM deposition [5,9,34–37]. In this context, our study identified CBG as a novel direct AMPK activator. Moreover, we showed that CBG inhibited fibrogenesis indirectly, through its anti-inflammatory effects in hepatocytes that subsequently impact HSC activation. These findings highlight the need for further investigation into the direct pharmacological effects of CBG on other liver-resident cell types, including HSCs, Kupffer cells, and liver sinusoidal endothelial cells.

CBG, a non-psychoactive minor phytocannabinoid with a distinct pharmacological profile [11], has been previously reported to exert anti-inflammatory effects by modulating redox balance and inhibiting NF-κB signaling [38]. In this study, we provide the first evidence that CBG directly activates AMPK, revealing a novel mechanism underlying its anti-inflammatory and metabolic actions. Beyond AMPK, CBG may exert additional effects through interaction with other molecular targets, including TRPV1, PPAR, FAAH, CB1, and CB2, which are key receptors and enzymes within the endocannabinoid system (ECS). Although the role of the ECS in liver fibrosis is complex and not yet fully understood [39], several studies have suggested that CB1 receptor activation promotes lipogenesis [40], while CB2 activation may exert protective effects on metabolic regulation [41]. Furthermore, CB ligands have been shown to regulate the expression of CB1 and CB2 receptors in an NF-κB-dependent manner [42]. These findings suggest that the antifibrotic activity of CBG may extend beyond AMPK activation, potentially involving both direct and indirect effects on the ECS. Future studies are warranted to delineate the broader molecular targets of CBG and their contributions to liver pathophysiology.

In investigations examining the effects of cannabidiol (CBD) and CBG, both individually and in combination, CBG demonstrated anti-inflammatory activity in the lungs by effectively modulating LPS-induced neutrophil infiltration [43]. Additionally, CBG has been reported to exhibit stronger anti-inflammatory effects in the skin compared to CBD [44], and derivatives of CBG have also shown potent anti-inflammatory properties [45]. Building on these findings, our study newly elucidated that CBG's anti-inflammatory activity is mediated

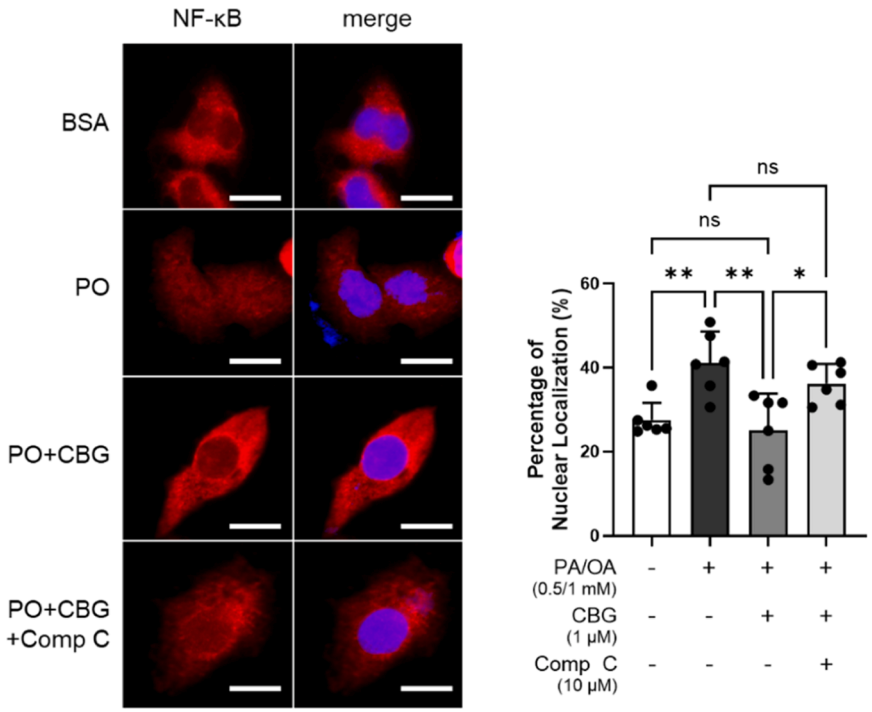


Fig. 8. CBG inhibited inflammatory signaling via AMPK-NF-κB axis. Immunofluorescence analysis of NF-κB nuclear translocation in HepG2 cells treated with PA/OA, CBG (1 or 10 μM), and/or compound C (10 μM). NF-κB is shown in red, and nuclei are counterstained with DAPI (blue). Scale bars = 20 μm. The intensity of nuclear localized NF-κB was quantified using Zen pro software. *p*-values were calculated using one-way ANOVA, followed by Tukey's multiple comparison test. $*p < 0.05$; $**p < 0.01$; ns., not significant. Data are presented as mean ± SD (n = 6 biological replicates).

through AMPK activation.

CBG is known to interact with multiple molecular targets, including cannabinoid receptors (CB_1 and CB_2), members of the TRPV family, and PPARγ [46]. This wide range of target profile may contribute to its hepatoprotective and anti-fibrotic effects through complementary mechanisms. Specifically, CBG has been reported to act as a weak partial antagonist of CB_1 and a weak agonist of CB_2 [47]. Given that both CB_1 blockade and CB_2 stimulation are associated with anti-fibrotic effects, the pharmacological activity of CBG on cannabinoid receptors also account for its hepatoprotective properties [48,49]. In addition, CBG has been reported to activate PPARγ, a nuclear receptor that plays a key role in regulating anti-inflammatory responses [50]. Given the known role of PPARγ in attenuating hepatic inflammation and fibrogenesis, its activation by CBG may further contribute to the observed therapeutic effects. Among these various molecular targets, our study newly identifies AMPK as a direct molecular target of CBG and highlights its central role in mediating the hepatoprotective effects of CBG.

One limitation of this study is that CBG did not induce significant changes in lipolysis under the experimental conditions. This may be due to the specific fatty acid loading model used, which may not have been optimal for detecting changes in lipolysis-related gene expressions. For this reason, we cannot conclusively determine the effect of CBG on lipolysis. Rather than indicating a lack of activity, our findings suggest that the therapeutic effects of CBG on hepatic lipid metabolism are predominantly mediated through its modulation of lipogenesis and lipophagy. Although this study demonstrated the effects of CBG using hepatocyte and HSC cell lines as well as a hepatic spheroid model, these *in vitro* systems do not fully recapitulate the complex multicellular and immunological microenvironment of fibrotic liver tissue *in vivo*. Therefore, the translational relevance of our findings requires further validation in physiologically relevant animal models of chronic liver injury. While previous reports have suggested the involvement of AMPK in the effects of cannabis extracts containing CBG, this study is the first to demonstrate that CBG directly binds to AMPK and activates its kinase activity. This novel finding provides new insights into the mechanistic underpinnings of CBG's protective effects against liver fibrosis and supports further development of CBG as a promising therapeutic agent.

The involvement of AMPK in anti-fibrotic activity of CBG was confirmed by experiments using compound C, a well-known AMPK inhibitor. However, it is important to note that compound C exhibits broader pharmacological activities beyond AMPK suppression. For instance, it has been reported to suppress HIF-1α activation [51], disrupt the unfolded protein response (UPR) transcriptional program [52], and inhibit a range of other protein kinases, including ERK8, MNK1, PHK, MELK, several DYRK isoforms, HIPK2, Src, Lck, Yes, FGFR1, and EphA2 [53]. These pleiotropic effects highlight the need for caution in interpreting results based solely on its use. To address this limitation, we did not rely solely on this pharmacological inhibition. While the reversal of the effects of CBG by compound C supports the involvement of AMPK, we further confirmed direct target engagement through an *in vitro* SAMS kinase assay using recombinant AMPK. This cell-free assay demonstrated that CBG directly activates AMPK, independent of upstream signaling pathways, thereby providing more specific evidence for AMPK as a molecular target of CBG.

Although a definitive conversion between *in vitro* concentrations and *in vivo* doses is not established, the effective *in vitro* concentrations used in this study (1–10 μM) approximately correspond to *in vivo* doses of 1.27–12.67 mg/kg, based on theoretical extrapolation using molecular wight of CBG and volume of distribution in mice. These estimates are comparable to dosing ranges reported in previous *in vivo* study (2.46–24.6 mg/kg/day, i.p.), supporting the translational relevance of our results [13].

In conclusion, our finding reveals a novel role for CBG as a direct AMPK activator that mitigates liver fibrosis by modulating lipid metabolism and inflammatory signaling. Collectively, our findings support the therapeutic potential of CBG as a novel antifibrotic agent. Future studies should focus on elucidating the cell type-specific effects of CBG within the liver, exploring its interactions with additional signaling pathways, and evaluating its efficacy and safety in clinically relevant *in vivo* models of chronic liver disease.

CRediT authorship contribution statement

Hwa Jong Lee: Investigation. **Tae Hyung Kim:** Investigation. **Eun Seon Pak:** Writing – review & editing, Investigation. **Soomin Kim:** Investigation. **Woong Jin Bae:** Writing – review & editing. **Sae Woong Kim:** Writing – review & editing, Funding acquisition. **Jun Jie Piao:** Investigation. **Dongho Shin:** Writing – review & editing. **Youngjoo Kwon:** Writing – review & editing, Supervision, Funding acquisition, Conceptualization. **Seojeong Kim:** Visualization, Investigation. **Seojeong Park:** Writing – review & editing, Investigation. **Kyung-Hwa Jeon:** Writing – original draft, Visualization, Validation, Investigation, Conceptualization.

Declaration of Competing Interest

The authors declare that they have no known competing financial interests or personal relationships that could have appeared to influence the work reported in this paper.

Acknowledgements

We gratefully acknowledge financial support from the National Research Foundation (NRF) (NRF-2022R1A2C2092053 and RS-2024-00431505) funded by the Ministry of Science and ICT (MSIT, Korea) and the Starting Growth Technological R&D Program (TIPS Program, RS-2023-00285144) funded by the Ministry of SMEs and Startups (MSS, Korea) in 2023, as well as the Research Fund of Catholic Integrative Medicine Research Institute, The Catholic University of Korea. The authors thank the Ewha Drug Development Research Core Center for their help with the CFX96 RT-PCR, Apotome laser-scanning microscope, and Infinite M200 PRO Microplate Reader analyses. K.H. Jeon was supported by RP-Grant 2024 of Ewha Womans University.

Appendix A. Supporting information

Supplementary data associated with this article can be found in the online version at doi:10.1016/j.biopha.2025.118463.

Data availability

No data was used for the research described in the article.

References

[1] H. Jia, J. Liu, T. Fang, Z. Zhou, R. Li, W. Yin, et al., The role of altered lipid composition and distribution in liver fibrosis revealed by multimodal nonlinear optical microscopy, Sci. Adv. 9 (2) (2023) eabq2937, https://doi.org/10.1126/sciadv.abq2937.
[2] V. Hernandez-Gea, S.L. Friedman, Pathogenesis of liver fibrosis, Annu Rev. Pathol. 6 (2011) 425–456, https://doi.org/10.1146/annurev-pathol-011110-130246.
[3] T. Kisseleva, D. Brenner, Molecular and cellular mechanisms of liver fibrosis and its regression, Nat. Rev. Gastroenterol. Hepatol. 18 (3) (2021) 151–166, https://doi.org/10.1038/s41575-020-00372-7.
[4] Z. Tan, H. Sun, T. Xue, C. Gan, H. Liu, Y. Xie, et al., Liver fibrosis: therapeutic targets and advances in drug therapy, Front. Cell Dev. Biol. 9 (2021) 730176, https://doi.org/10.3389/fcell.2021.730176.
[5] H. An, Y. Jang, J. Choi, J. Hur, S. Kim, Y. Kwon, New insights into AMPK, as a potential therapeutic target in metabolic dysfunction-associated steatotic liver disease and hepatic fibrosis, Biomol. Ther. (Seoul) 33 (1) (2025) 18–38, https://doi.org/10.4062/biomolther.2024.188.
[6] J. Zhang, Y. Li, Q. Liu, Y. Huang, R. Li, T. Wu, et al., Sirt6 alleviated liver fibrosis by deacetylating conserved lysine 54 on Smad2 in hepatic stellate cells, Hepatology 73 (3) (2021) 1140–1157, https://doi.org/10.1002/hep.31418.
[7] J. Zhang, Q. Liu, J. He, Y. Li, Novel therapeutic targets in liver fibrosis, Front. Mol. Biosci. 8 (2021) 766855, https://doi.org/10.3389/fmolb.2021.766855.
[8] J. Shinn, S. Park, S. Lee, N. Park, S. Kim, S. Hwang, et al., Antioxidative hyaluronic acid-bilirubin nanomedicine targeting activated hepatic stellate cells for anti-hepatic-fibrosis therapy, ACS Nano 18 (6) (2024) 4704–4716, https://doi.org/10.1021/acsnano.3c06107.
[9] S. Kim, J.H. Shin, M. Seo, E.S. Pak, K.H. Jeon, I. Moon, J. Kang, W. Seo, Y. Na, Y. Kwon, Pharmacological activation of AMP-activated protein kinase ameliorates liver fibrosis in a metabolic dysfunction-associated steatohepatitis mouse model, Int. J. Biol. Sci. 21 (7) (2025) 2957–2972.
[10] S. Park, S. Hwang, J. Sun, K.H. Jeon, N. Sheen, S. Shin, et al., A novel A2a adenosine receptor inhibitor effectively mitigates hepatic fibrosis in a metabolic dysfunction-associated steatohepatitis mouse model, Int. J. Biol. Sci. 20 (5) (2024) 1855–1870, https://doi.org/10.7150/ijbs.92371.
[11] R. Nachnani, W.M. Raup-Konsavage, K.E. Vrana, The pharmacological case for cannabigerol, J. Pharm. Exp. Ther. 376 (2) (2021) 204–212, https://doi.org/10.1124/jpet.120.000340.
[12] T. Gülck, B.L. Møller, Phytocannabinoids: origins and biosynthesis, Trends Plant Sci. 25 (10) (2020) 985–1004, https://doi.org/10.1016/j.tplants.2020.05.005.
[13] N. Aljobaily, K. Krutsinger, M.J. Viereckl, R. Joly, B. Menlove, B. Cone, et al., Low-Dose administration of cannabigerol attenuates inflammation and fibrosis associated with methionine/choline deficient diet-induced NASH model via modulation of cannabinoid receptor, Nutrients 15 (1) (2022), https://doi.org/10.3390/nu15010178.
[14] D. Garcia, R.J. Shaw, AMPK: mechanisms of cellular energy sensing and restoration of metabolic balance, Mol. Cell 66 (6) (2017) 789–800, https://doi.org/10.1016/j.molcel.2017.05.032.
[15] A. Cittadini, R. Napoli, M.G. Monti, D. Rea, S. Longobardi, P.A. Netti, et al., Metformin prevents the development of chronic heart failure in the SHHF rat model, Diabetes 61 (4) (2012) 944–953, https://doi.org/10.2337/db11-1132.
[16] Y. Li, S. Xu, M.M. Mihaylova, B. Zheng, X. Hou, B. Jiang, et al., AMPK phosphorylates and inhibits SREBP activity to attenuate hepatic steatosis and atherosclerosis in diet-induced insulin-resistant mice, Cell Metab. 13 (4) (2011) 376–388, https://doi.org/10.1016/j.cmet.2011.03.009.
[17] J. Kim, G. Yang, Y. Kim, J. Kim, J. Ha, AMPK activators: mechanisms of action and physiological activities, Exp. Mol. Med. 48 (4) (2016) e224, https://doi.org/10.1038/emm.2016.16.
[18] R. DeFronzo, G.A. Fleming, K. Chen, T.A. Bicsak, Metformin-associated lactic acidosis: current perspectives on causes and risk, Metabolism 65 (2) (2016) 20–29, https://doi.org/10.1016/j.metabol.2015.10.014.
[19] B. Xiao, M.J. Sanders, D. Carmena, N.J. Bright, L.F. Haire, E. Underwood, et al., Structural basis of AMPK regulation by small molecule activators, Nat. Commun. 4 (2013) 3017, https://doi.org/10.1038/ncomms4017.
[20] L. Hammerich, F. Tacke, Hepatic inflammatory responses in liver fibrosis, Nat. Rev. Gastroenterol. Hepatol. 20 (10) (2023) 633–646, https://doi.org/10.1038/s41575-023-00807-x.
[21] X. Cai, J. Wang, J. Wang, Q. Zhou, B. Yang, Q. He, et al., Intercellular crosstalk of hepatic stellate cells in liver fibrosis: new insights into therapy, Pharm. Res. 155 (2020) 104720, https://doi.org/10.1016/j.phrs.2020.104720.
[22] B. Dewidar, C. Meyer, S. Dooley, A.N. Meindl-Beinker, TGF-β in hepatic stellate cell activation and liver fibrogenesis-updated 2019, Cells 8 (11) (2019), https://doi.org/10.3390/cells8111419.
[23] S. Wang, H. Li, M. Yuan, H. Fan, Z. Cai, Role of AMPK in autophagy, Front. Physiol. 13 (2022) 1015500, https://doi.org/10.3389/fphys.2022.1015500.
[24] Z. Liang, T. Li, S. Jiang, J. Xu, W. Di, Z. Yang, et al., AMPK: a novel target for treating hepatic fibrosis, Oncotarget 8 (37) (2017) 62780–62792, https://doi.org/10.18632/oncotarget.19376.
[25] T. Assa-Glazer, J. Gorelick, N. Sela, A. Nyska, N. Bernstein, Z. Madar, Cannabis extracts affected metabolic syndrome parameters in mice fed High-Fat/Cholesterol diet, Cannabis Cannabinoid Res. 5 (3) (2020) 202–214, https://doi.org/10.1089/can.2020.0013.
[26] B. Cool, B. Zinker, W. Chiou, L. Kifle, N. Cao, M. Perham, et al., Identification and characterization of a small molecule AMPK activator that treats key components of type 2 diabetes and the metabolic syndrome, Cell Metab. 3 (6) (2006) 403–416, https://doi.org/10.1016/j.cmet.2006.05.005.
[27] Y. Si, J. Wang, X. Liu, T. Zhou, Y. Xiang, T. Zhang, et al., Ethoxysanguinarine, a novel direct activator of AMP-Activated protein kinase, induces autophagy and exhibits therapeutic potential in breast cancer cells, Front. Pharm. 10 (2019) 1503, https://doi.org/10.3389/fphar.2019.01503.
[28] T. Luedde, R.F. Schwabe, NF-κB in the liver–linking injury, fibrosis and hepatocellular carcinoma, Nat. Rev. Gastroenterol. Hepatol. 8 (2) (2011) 108–118, https://doi.org/10.1038/nrgastro.2010.213.
[29] A. Salminen, J.M. Hyttinen, K. Kaarniranta, AMP-activated protein kinase inhibits NF-κB signaling and inflammation: impact on healthspan and lifespan, J. Mol. Med. (Berl.) 89 (7) (2011) 667–676, https://doi.org/10.1007/s00109-011-0748-0.
[30] J.Y. Lim, M.A. Oh, W.H. Kim, H.Y. Sohn, S.I. Park, AMP-activated protein kinase inhibits TGF-β-induced fibrogenic responses of hepatic stellate cells by targeting transcriptional coactivator p300, J. Cell Physiol. 227 (3) (2012) 1081–1089, https://doi.org/10.1002/jcp.22824.
[31] P. Kumar, T. Smith, K. Rahman, N.E. Thorn, F.A. Anania, Adiponectin agonist ADP355 attenuates CCl4-induced liver fibrosis in mice, PLoS One 9 (10) (2014) e110405, https://doi.org/10.1371/journal.pone.0110405.
[32] Y. Yang, Z. Zhao, Y. Liu, X. Kang, H. Zhang, M. Meng, Suppression of oxidative stress and improvement of liver functions in mice by ursolic acid via LKB1-AMP-activated protein kinase signaling, J. Gastroenterol. Hepatol. 30 (3) (2015) 609–618, https://doi.org/10.1111/jgh.12723.
[33] P.H. Pan, S.Y. Lin, Y.Y. Wang, W.Y. Chen, Y.H. Chuang, C.C. Wu, et al., Protective effects of rutin on liver injury induced by biliary obstruction in rats, Free Radic. Biol. Med. 73 (2014) 106–116, https://doi.org/10.1016/j.freeradbiomed.2014.05.001.
[34] H. Wang, H. Zhang, Y. Zhang, D. Wang, X. Cheng, F. Yang, et al., Plumbagin protects liver against fulminant hepatic failure and chronic liver fibrosis via inhibiting inflammation and collagen production, Oncotarget 7 (50) (2016) 82864–82875, https://doi.org/10.18632/oncotarget.12655.

[35] A. da Silva Morais, J. Abarca-Quinones, B. Guigas, B. Viollet, P. Stärkel, Y. Horsmans, et al., Development of hepatic fibrosis occurs normally in AMPK-deficient mice, Clin. Sci. (Lond.) 118 (6) (2009) 411–420, https://doi.org/10.1042/cs20090293.
[36] J. Li, Y. Pan, M. Kan, X. Xiao, Y. Wang, F. Guan, et al., Hepatoprotective effects of berberine on liver fibrosis via activation of AMP-activated protein kinase, Life Sci. 98 (1) (2014) 24–30, https://doi.org/10.1016/j.lfs.2013.12.211.
[37] M. Ramezani-Moghadam, J. Wang, V. Ho, T.J. Iseli, B. Alzahrani, A. Xu, et al., Adiponectin reduces hepatic stellate cell migration by promoting tissue inhibitor of metalloproteinase-1 (TIMP-1) secretion, J. Biol. Chem. 290 (9) (2015) 5533–5542, https://doi.org/10.1074/jbc.M114.598011.
[38] A. Gugliandolo, F. Pollastro, G. Grassi, P. Bramanti, E. Mazzon, In vitro model of neuroinflammation: efficacy of cannabigerol, a non-psychoactive cannabinoid, Int. J. Mol. Sci. 19 (7) (2018), https://doi.org/10.3390/ijms19071992.
[39] P. Melgar-Lesmes, M. Perramon, W. Jiménez, Roles of the hepatic endocannabinoid and apelin systems in the pathogenesis of liver fibrosis, Cells 8 (11) (2019), https://doi.org/10.3390/cells8111311.
[40] D. Osei-Hyiaman, M. DePetrillo, P. Pacher, J. Liu, S. Radaeva, S. Bátkai, et al., Endocannabinoid activation at hepatic CB1 receptors stimulates fatty acid synthesis and contributes to diet-induced obesity, J. Clin. Invest. 115 (5) (2005) 1298–1305, https://doi.org/10.1172/jci23057.
[41] P. Morales, L. Hernandez-Folgado, P. Goya, N. Jagerovic, Cannabinoid receptor 2 (CB2) agonists and antagonists: a patent update, Expert Opin. Ther. Pat. 26 (7) (2016) 843–856, https://doi.org/10.1080/13543776.2016.1193157.
[42] M. Donadelli, I. Dando, T. Zaniboni, C. Costanzo, E. Dalla Pozza, M.T. Scupoli, et al., Gemcitabine/cannabinoid combination triggers autophagy in pancreatic cancer cells through a ROS-mediated mechanism, Cell Death Dis. 2 (4) (2011) e152, https://doi.org/10.1038/cddis.2011.36.
[43] C.L. Robaina Cabrera, S. Keir-Rudman, N. Horniman, N. Clarkson, C. Page, The anti-inflammatory effects of cannabidiol and cannabigerol alone, and in combination, Pulm. Pharm. Ther. 69 (2021) 102047, https://doi.org/10.1016/j.pupt.2021.102047.
[44] E. Perez, J.R. Fernandez, C. Fitzgerald, K. Rouzard, M. Tamura, C. Savile, In vitro and clinical evaluation of cannabigerol (CBG) produced via yeast biosynthesis: a cannabinoid with a broad range of anti-inflammatory and skin health-boosting properties, Molecules 27 (2) (2022), https://doi.org/10.3390/molecules27020491.
[45] N.M. Kogan, Y. Lavi, L.M. Topping, R.O. Williams, F.E. McCann, Z. Yekhtin, et al., Novel CBG derivatives can reduce inflammation, pain and obesity, Molecules 26 (18) (2021), https://doi.org/10.3390/molecules26185601.
[46] S. Li, W. Li, N.K. Malhi, J. Huang, Q. Li, Z. Zhou, et al., Cannabigerol (CBG): a comprehensive review of its molecular mechanisms and therapeutic potential, Molecules 29 (22) (2024), https://doi.org/10.3390/molecules29225471.
[47] M.F. Mahmoud, S.E. Swefy, R.A. Hasan, A. Ibrahim, Role of cannabinoid receptors in hepatic fibrosis and apoptosis associated with bile duct ligation in rats, Eur. J. Pharm. 742 (2014) 118–124, https://doi.org/10.1016/j.ejphar.2014.08.021.
[48] A. Mallat, F. Teixeira-Clerc, S. Lotersztajn, Cannabinoid signaling and liver therapeutics, J. Hepatol. 59 (4) (2013) 891–896, https://doi.org/10.1016/j.jhep.2013.03.032.
[49] F. Teixeira-Clerc, B. Julien, P. Grenard, J. Tran Van Nhieu, V. Deveaux, L. Li, et al., CB1 cannabinoid receptor antagonism: a new strategy for the treatment of liver fibrosis, Nat. Med. 12 (6) (2006) 671–676, https://doi.org/10.1038/nm1421.
[50] H. Chen, H. Tan, J. Wan, Y. Zeng, J. Wang, H. Wang, et al., PPAR-γ signaling in nonalcoholic fatty liver disease: pathogenesis and therapeutic targets, Pharm. Ther. 245 (2023) 108391, https://doi.org/10.1016/j.pharmthera.2023.108391.
[51] B.M. Emerling, B. Viollet, K.V. Tormos, N.S. Chandel, Compound c inhibits hypoxic activation of HIF-1 independent of AMPK, FEBS Lett. 581 (29) (2007) 5727–5731, https://doi.org/10.1016/j.febslet.2007.11.038.
[52] S. Saito, A. Furuno, J. Sakurai, H.R. Park, K. Shin-ya, A. Tomida, Compound c prevents the unfolded protein response during glucose deprivation through a mechanism independent of AMPK and BMP signaling, PLoS One 7 (9) (2012) e45845, https://doi.org/10.1371/journal.pone.0045845.
[53] J. Bain, L. Plater, M. Elliott, N. Shpiro, C.J. Hastie, H. McLauchlan, et al., The selectivity of protein kinase inhibitors: a further update, Biochem. J. 408 (3) (2007) 297–315, https://doi.org/10.1042/bj20070797.